

MONITORING OF PHASE JITTER IN FIBRE OPTIC TIME AND FREQUENCY TRANSFER SYSTEMS

Karol Salwik, Łukasz Śliwczyński, Przemysław Krehlik

AGH University of Science and Technology, Faculty of Computer Science, Electronics and Telecommunications,
Al. A. Mickiewicza 30, 30-059 Cracow, Poland (✉ salwik@agh.edu.pl, 48 12 617 3020, sliwczyn@agh.edu.pl,
krehlik@agh.edu.pl)

Abstract

The phase jitter enables to assess quality of signals transmitted in a bi-directional, long-distance fibre optic link dedicated for dissemination of the time and frequency signals. In the paper, we are considering measurements of jitter using a phase detector the detected frequency signal and the reference signal are supplied to. To cover the wideband jitter spectrum the detected signal frequency is divided and – because of the aliasing process – higher spectral components are shifted down. We are also examining the influence of a residual jitter that occurs in the reference signal generated by filtering the jitter occurring in the same signal, whose phase fluctuations we intend to measure. Then, we are discussing the evaluation results, which were obtained by using the target fibre optic time and frequency transfer system.

Keywords: jitter measurement, phase comparison, fibre optics, time and frequency transfer, bidirectional optical amplifier.

© 2018 Polish Academy of Sciences. All rights reserved

1. Introduction

Fibre optic transfer of *time and frequency* (T&F) signals is nowadays considered as a technique offering the highest potential concerning accuracy and stability [1–4]. This is because the bi-directional transmission in a single fibre, thanks to the inherent symmetry of propagation conditions in opposite directions, enables efficient elimination of noise generated in the fibre due to temperature fluctuations and mechanical vibration [5–6]. When it has become apparent that satellite signals might be easily jammed or spoofed, the fibre optic distribution is also acknowledged to be a real alternative to ubiquitous satellite transfer techniques [7].

The transfer system considered in the paper is assumed to transmit time and frequency signals via a fibre optic link to a remote location. A general block diagram of the system with its main components marked on is shown in Fig. 1.

A very stable electrical frequency signal, derived from a caesium source or a hydrogen maser with a typical frequency of 5 MHz or 10 MHz, is supplied to the local module where it is converted into a square wave with a rise/fall time of ~100 ps. The optional timestamp (*e.g.* 1 pulse per second – PPS) is superimposed as violation of the duty cycle. Such a signal is used to modulate the intensity of a semiconductor laser using external *electro-absorption modulator* (EAM)

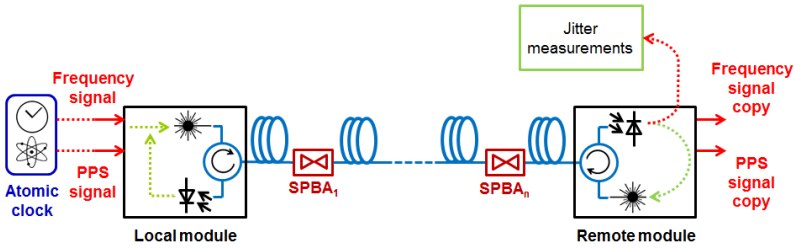


Fig. 1. A block diagram of the T&F transfer system.

and then it is transferred via the fibre optic link. In the remote module the optical signal is directly detected by comparing the photodiode output with a threshold value.

The transmission distance of an unamplified bi-directional fibre optic T&F transfer system depends on many factors. Some of them, such as fibre losses, weaken the optical signal, while the others (e.g. Rayleigh backscattering or conversion of the laser phase noise into an intensity noise through the chromatic dispersion of the fibre) increase noise in the link [8–10]. The distance may be extended using special *single-path bidirectional amplifiers* (SPBA) based on an erbium-doped fibre, which compensates the losses and do not disturb the link forward-backward symmetry. However, the optical amplifiers generate additional noise, resulting from *amplified spontaneous emission* (ASE). Because of the link bi-directionality, they amplify the backscattered signals as well. Thus, the gains of SPBAs need to be judiciously adjusted to compensate losses, and also to minimize undesirable effects [11].

A gain optimization procedure may be performed manually, where gains of the amplifiers are pre-set basing on the simulation results [12]. This procedure is only an approximation. It is impossible to determine all the parameters describing the fibre optic link and predict the influence of the environmental factors that would enable to model the accurate operating conditions [13]. It is also cumbersome to verify in practice whether the settings of the SPBAs are really optimal. Thus, to provide continuous optimum performance, the real-time monitoring of the link performance is necessary. Measurements of the phase fluctuations (jitter) of the transmitted frequency signal enable to estimate its quality and observe the influence of a potential SPBA's gain correction. This correction can increase or reduce noise in the link, causing corresponding changes of the jitter. Moreover, it is not necessary to find out the particular sources of the noise that degrades the transmitted signal's quality for the SPBA gain optimization procedure.

The jitter occurring in the discussed T&F transfer system can be measured as the phase changes of the transmitted signal related to the jitter-free reference signal. To make the measurements possible at any point of a long-distance link (e.g. in the remote module), the reference need to be locally generated. It is done using a *phase locked loop* (PLL) that filters out the jitter occurring in transmitted frequency signal (the same signal whose jitter we intend to measure). However, such a reference contains a residual jitter, as it is impossible to filter out all the phase fluctuations. This residual jitter is expected to be much lower than the jitter we intend to measure.

The jitter may be directly visualized using e.g. a high-speed oscilloscope triggered with the reference signal and fed with the detected transmitted signal. The oscilloscope enables to observe the phase difference between its input signals. However, this measurement method is unpractical for the continuous operation in a real long-distance link. Another approach, adopted in the work, is to use a frequency mixer operating as the phase detector. As in the case of the oscilloscope

measurements, the phase detector is supplied with the jittered signal and the reference signal. The *root-mean-square* (RMS) value of its output voltage is proportional to the jitter [14] and is sufficient for the SPBA gain optimization.

In this paper we present the general idea of jitter measurement (Section 2) and its practical implementation (Section 3). The *jitter measurement unit* (JMU) has been widely tested including its evaluation in the target bi-directional fibre optic T&F transfer system. The results of these measurements are presented in Section 4.

2. Jitter measurement using phase detector

The considered jitter measurement method uses a frequency mixer followed by a *low-pass filter* (LPF) operating as the phase detector [15–16]. The mixer is fed with a jitter-corrupted signal and a reference with a residual jitter. Both signals need to be in quadrature. The jitter may be described as instantaneous phase fluctuations of the supplied signals – $\varphi_1(t)$ and $\varphi_2(t)$, respectively [17]. The magnitude of LPF output is linearly proportional to the jitter:

$$O_{LPF}(t) \propto \varphi_1(t) - \varphi_2(t). \quad (1)$$

$\varphi_1(t)$ is expected to have the dominant influence on the RMS value of LPF output voltage. However, as the jitter is relatively small (with a value of picoseconds), $O_{LPF}(t)$ is very small, providing an additional level of difficulty for its measurement. One possible method for increasing this voltage is multiplication of the frequency of the signals supplied to the phase detector [18]. This operation does not change the jitter in the time domain (it is still a few picoseconds), but multiplies it in radians (*i.e.* in relation to the signal period). For a typical frequency signal (*e.g.* 10 MHz derived from the caesium time/frequency standard) the proportion of the jitter to the signal period is like a few picoseconds to 100 ns. After the multiplication up to 1 GHz, this proportion is like a few picoseconds to 1 ns. As a result of that, the RMS value of LPF output voltage is higher.

3. Jitter measurement unit

A general scheme of the proposed measurement solution is shown in Fig. 2. The JMU consists of four main functional blocks – the jitter cleaner, the jitter tracker (both constructed using PLL circuits), the phase detector (the frequency mixer and the LPF) and the RMS voltmeter.

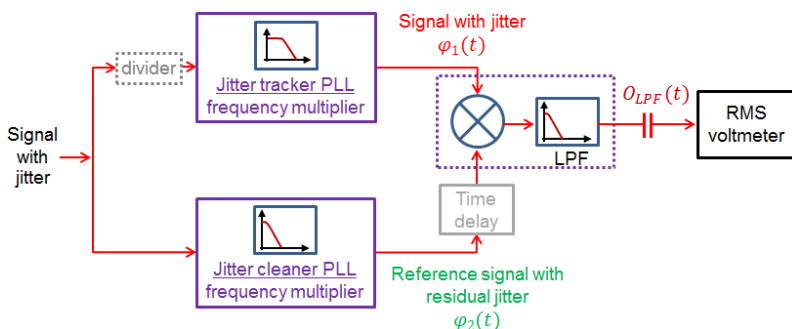


Fig. 2. A general block diagram of the proposed measurement solution. See description in the text.

3.1. Functional blocks

The jitter cleaner PLL produces the reference signal for the jitter measurements. The PLL is fed with the detected frequency signal transmitted through the fibre optic link and filters out its jitter (the loop bandwidth is narrow). As it is desirable to measure the jitter in a high-frequency signal (see Section 2 for details), the jitter cleaner PLL provides also the frequency multiplication.

The jitter tracker PLL also multiplies its input frequency, but does not affect the jitter occurring in this signal. For this reason the loop filter bandwidth needs to correspond to the jitter spectrum. This spectrum is expected to be wide, as the jitter results from the wide-band noise generated in the fibre. To avoid the situation that the bandwidth of the PLL does not cover the whole jitter spectrum (e.g. because of hardware limitations), the frequency of the tracker input signal is divided. As this process is synchronous with the signal affected by jitter, the phase fluctuations are transferred to the divided signal. If we also notice that some jitter-corrupted slopes are discarded, we may consider it as sampling of the jitter [19]. Thus, its spectrum is limited to half of the divided signal frequency, above which the aliasing occurs, moving higher spectral components down.

On the other hand, the dividing process of the jitter-corrupted signal and its influence on the jitter measurements may be explained using statistical reasoning. If we would take the noise as a random process, the RMS value (by the same token – the jitter) may be interpreted as its standard deviation [20]. Using only the samples of this random process, it is possible to estimate its standard deviation [21].

The signals from both the jitter tracker and the jitter cleaner are supplied to the double-balanced mixer that operates as a phase detector. For the proper operation, the signals need to be in quadrature (the phase shift between them is 1/4 of the signal period), thus the delay is provided by the “Time delay” block. After the phase detection (multiplication in the mixer and filtration in the LPF), the obtained voltage is supplied to the RMS meter (in principle an RMS-to-DC converter). The AC-coupling is used to cut-off the DC component of $O_{LPF}(t)$ which occurs if the mixer input signals are not exactly in quadrature. Such a component contains no information about the jitter, and has to be removed. The RMS voltage is proportional to the jitter and can be used in further processing (particularly for optimizing the T&F link performance by minimizing the jitter).

3.2. Practical implementation

In practical implementation, we decided to use Texas Instruments LMK03033C PLL integrated circuits for both – jitter cleaner and jitter tracker – applications. These circuits provide low additional phase noise (jitter below 1 ps) and contain all necessary components (except for a complete loop filter) in a single chip.

The jitter cleaner is expected to filter out the wide-band jitter to obtain the reference signal for the measurements, thus its bandwidth needs to be narrow. In general, limiting the bandwidth of the PLL too much increases the influence of the internal phase noise of the *voltage control oscillator* (VCO) on the output jitter [22], so a compromise is necessary. A loop bandwidth of 5 kHz has been obtained based on simulations of the LMK03033C PLL.

When considering the jitter tracker, hardware limitations of the LMK03033C PLL circuit do not enable to implement the loop filter with a bandwidth greater than a few tens of kilohertz, which is insufficient for the proposed application. For the proper operation, the PLL input signal is divided down to 100 kHz and thus the jitter spectrum (and the required loop bandwidth) is limited to 50 kHz (see Subsection 3.1 for details).

4. Experimental results

The device has been evaluated in the laboratory to verify correctness of the measurement idea. The tests were divided into two parts, which included characterization (*i.e.* assessment of the basic circuit parameters) and measurements of the JMU in the T&F transfer system, where the JMU is expected to operate. First, we checked whether the RMS value of the jitter was not changed because of the processes occurring in the JMU (particularly in the jitter tracker), as we assumed during the development. The assumption of the linear dependence of the RMS value of the jitter on the voltage retrieved from these phase fluctuations was also examined.

4.1. Transfer and frequency characteristics

The device characterization was done using signals with the known parameters (including parameters of generated noise). The signal with jitter was obtained as a combination of a square waveform and a jitter-generating signal (a sine wave or amplitude noise with a flat spectrum extending up to the frequency of around 100 MHz). This jitter-corrupted signal was supplied to the JMU and at the same time to a high-speed Agilent Infiniium 5855A oscilloscope, which enabled to visualize the jitter and verify the JMU measurement results. A general block diagram of the test-bench for this part of tests is shown in Fig. 3.

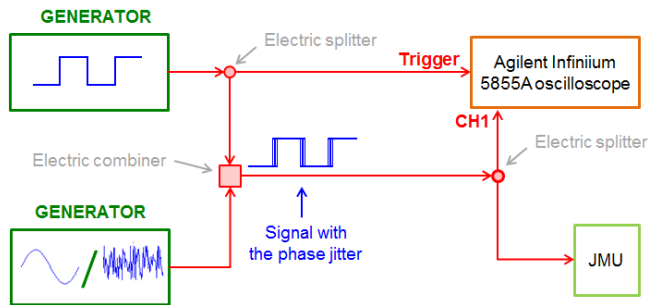


Fig. 3. A general block diagram of the test-bench.

First, the relationship between the signal phase jitter and the mixer output RMS voltage was examined. The transfer characteristic was measured for the jitter generated by both sine signal and noise. By changing the level of these signals, we were able to control the phase jitter occurring in the square waveform. The obtained transfer characteristics are shown in Fig. 4.

The tests were started with the minimum value of the signals generating jitter and were continued until the 50 ps jitter was obtained. The lowest jitter observed on the oscilloscope was about 2 ps, but because of the hardware limitations of the Analog Devices AD8361 RMS-to-DC converter used in the JMU, the minimal jitter that could be measured was 5 ps.

For either character of the jitter (jitter resulted from the sine signal or noise) the linear conversion was observed in the range of 5 ps to 50 ps. However, if the jitter results from the sine signal (Fig. 4a), the increase in the JMU output value is higher, than in the case of the jitter resulted from noise (Fig. 4b). This behaviour may be explained using the frequency characteristic of the JMU, measured in the next part of evaluation.

The frequency characteristic was obtained using the signal affected by jitter resulting from the sine voltage with a constant amplitude and a variable frequency. The response of the JMU

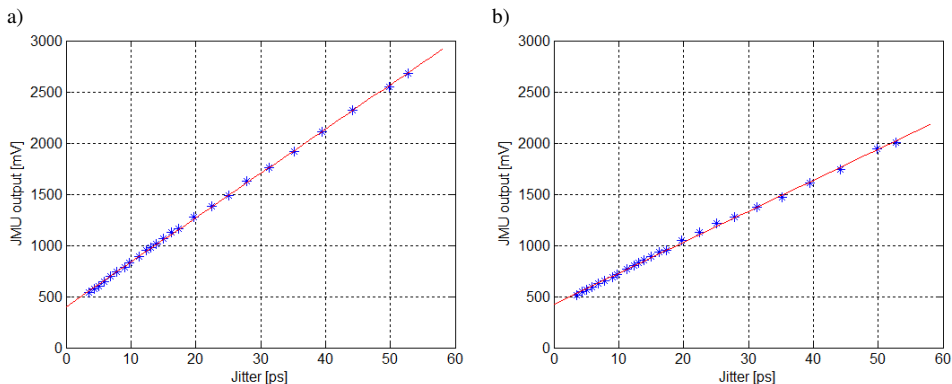


Fig. 4. JMU transfer characteristics – the JMU output voltage corresponding to the RMS jitter generated by a 9 kHz sine signal (a) and noise (b).

was measured in the range of 1 Hz to 5 MHz. The most important part of the obtained frequency characteristic is shown in Fig. 5, divided into two plots for a better visualization of the observed JMU response.

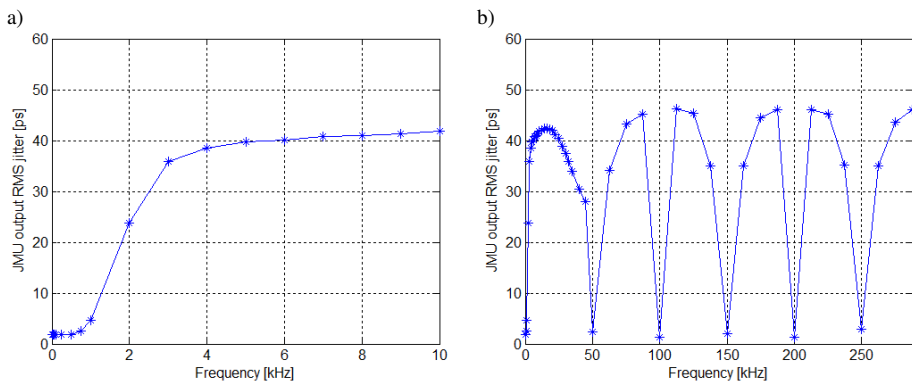


Fig. 5. The JMU frequency characteristic – divided into two plots for a better visualization of results. The JMU response observed in the range 50 kHz – 150 kHz repeats periodically up to 5 MHz.

The frequency characteristic shows that the JMU is unable to measure the jitter at some points. Thus, an effective slope of the transfer characteristic is influenced by the spectrum of the measured signal. A sinusoidal signal has the spectral power concentrated at a single frequency peak. Particularly, for the 9 kHz sine signal (used in measurements of the transfer characteristic shown in Fig. 4a) this peak is located in the range of frequencies where sensitivity is not reduced (Fig. 5a). On the other hand, the noise spectrum is spread and some of its components are omitted while measured by the JMU. For this reason, there is a difference between the slopes of the transfer characteristic measured for the jitter generated by the 9 kHz sine signal (Fig. 4a) and for the jitter generated by noise (Fig. 4b).

In order to explain the frequency characteristic, it is necessary to consider the impact of both PLL circuits that operate in parallel on the same signal supplied to the JMU. The bandwidth of the jitter cleaner is 5 kHz and thus the jitter spectral components in this range are passed. It is

particularly noticeable for the lowest frequencies (up to 1 kHz), where the phase fluctuations $\varphi_2(t)$ at the jitter cleaner output are not filtered out and are subtracted from the phase fluctuations $\varphi_1(t)$ passed by the jitter tracker (1). As a result, we observe reduction of the JMU sensitivity in the range of lowest frequencies.

For the frequencies above the bandwidth of the jitter cleaner, the phase fluctuations are filtered out and have no influence on the frequency response of the JMU. The deep peaks at 50 kHz, 100 kHz, 150 kHz, *etc.* result from the processes occurring in the jitter tracker PLL. We have taken these processes as the jitter sampling with a rate of 100 kHz (which results from dividing the tracker input signal frequency), thus the jitter tracker loop bandwidth is 50 kHz, above which the aliasing occurs. This feature creates the copies of the spectrum occurring around each integer multiple of the sampling frequency and – as a result – the high frequency components of the jitter spectrum are copied to the tracker bandwidth. However, the signals close to the bandwidth limit (50 kHz) are close to their aliased copy as well, and interfere with it. As a result, the JMU sensitivity is reduced at frequencies of 50 kHz, 150 kHz, *etc.*

The other effect, resulted from the aliasing, reduces sensitivity at 100 kHz, 200 kHz, *etc.* The spectral components close to these particular points are copied to the tracker baseband and occur near 0 Hz (DC). However, the RMS-to-DC converter is AC-coupled with the LPF output and it is unable to measure the RMS voltage in this range.

4.2. Measurements in target time and frequency transfer system

The second part of evaluation was performed in the target T&F transfer system, transmitting the frequency signal along a 300 km long fibre optic link with two bi-directional SPBAs installed every 100 km. It provided operating conditions close to the real ones for the JMU as the jitter resulted from the phenomena occurring in the link.

A block diagram of the measurement setup is shown in Fig. 6. A very stable frequency signal was supplied to the local module, and then transferred through a fibre optic link. By modifying gains of the SPBAs we were able to affect the link performance and thus to impose various jitter. After its detection in the remote module, the jitter-corrupted signal was supplied to the JMU and to the oscilloscope.

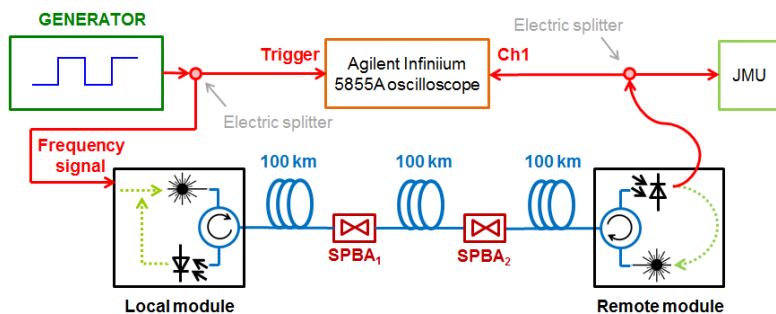


Fig. 6. JMU tests in T&F transfer systems – a simplified block diagram.

The total jitter in the transferred frequency signal comes from wide-band noise (resulted from the phenomena listed in Section 1) and low-pass narrowband noise (*e.g.* flicker noise). To examine the influence of the low-pass jitter, the outputs of jitter cleaner and the jitter tracker were observed separately on the oscilloscope. The gain of SPBA1 was held constant at 17.5 dB, while the gain of SPBA2 was swept in the range from 13 dB to 20 dB.

As it may be noted from the diagram presented in Fig. 7, the jitter measured at the cleaner PLL output is at least 10 ps lower than the jitter at the tracker PLL output. The changes of the amplifier gain have the minimal influence on the jitter-cleaner output signal. Thus we conclude that the low-pass narrowband components will not significantly affect the JMU performance in the considered application.

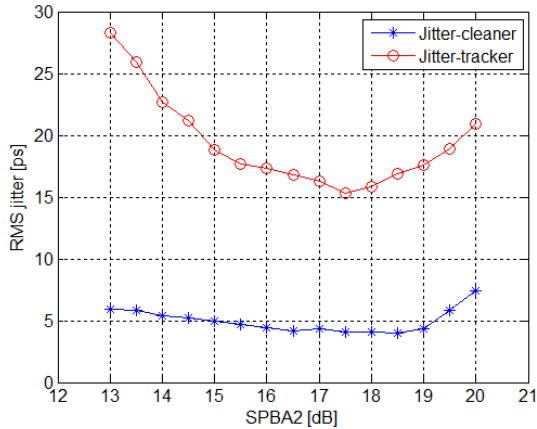


Fig. 7. The RMS jitter measured at the outputs of jitter cleaner and jitter tracker. The gain of SPBA1 was held constant at 17.5 dB.

In the next step, the jitter occurring in the transferred signal was measured by the JMU and visualized at the same time on the oscilloscope. The data collected during the test enabled to draw the characteristics (Fig. 8) of the RMS jitter as functions of gains of the optical amplifiers.

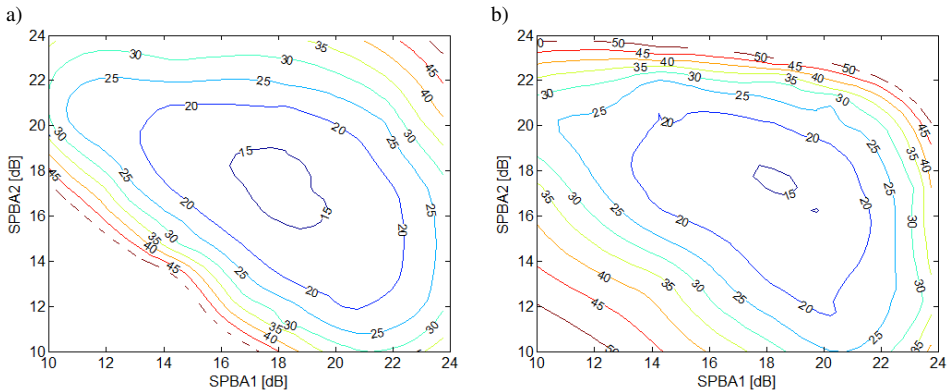


Fig. 8. T&F 300 km link performance – the RMS jitter measured by the oscilloscope (a) and by the JMU (b).

The results of the measurements performed with the JMU (Fig. 8b) are in agreement with the oscilloscope ones (Fig. 8a). Additionally, the characteristics were compared with the simulation results of an equivalent link. The simulator calculated the *signal to noise ratio* (SNR), which is inversely proportional to the jitter. The characteristic of SNR as a function of gains is shown in Fig. 9. It is difficult to calculate the jitter from SNR as the model does not include degradation

of the transferred signal, resulted from other factors than noise (*e.g.* chromatic dispersion) that occurs in a real fibre-optic link.

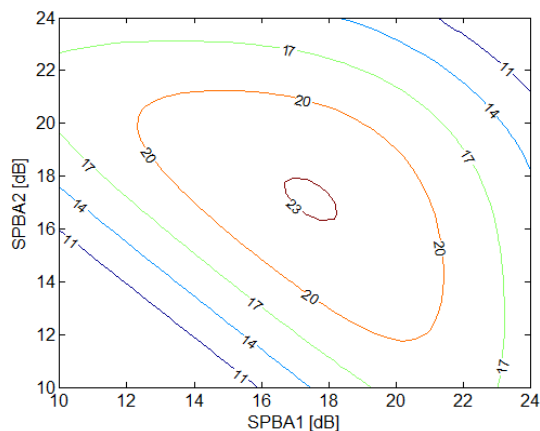


Fig. 9. The signal-to-noise ratio obtained from simulation of a 300 km long fibre optic link.

All of the characteristics clearly specify the area of optimal T&F system performance and the general trend of the parameter (jitter or SNR) changes is preserved. The JMU sensitivity is sufficient to indicate whether the gains of SPBAs need to be modified and what is the possible direction of such changes.

5. Conclusions

In the paper we presented the complete solution for monitoring of the phase jitter in a long-distance fibre optic T&F transfer system. Measurements of the phase fluctuations occurring in the transmitted frequency signal provide sufficient information to estimate the link performance. Based on this data, the real-time optimization by changing the setup of optical amplifiers can be performed.

The JMU compares phases of the jitter-corrupted signal and the reference signal. Such a reference could be the frequency signal from an atomic clock, supplied to the local module of T&F system. However, it would enable to measure the jitter at the link beginning only. To make the measurements possible at any point of the link (in principle in the remote module), the device contains the jitter-cleaner PLL circuit that filters out the jitter from the signal transferred through the link. Therefore, the JMU generates the reference with residual jitter, using the same signal whose phase fluctuations we intend to measure. In the proposed application, this minimal jitter has no significant influence on the measurement results.

The RMS value of the voltage (in fact the noise) obtained from the phase detector corresponds directly to the jitter. For typical frequency signals from an atomic source (*e.g.* 10 MHz) the jitter value of picoseconds is small compared with the signal period and thus the RMS voltage is small. The method for its amplification adopted in the work is the frequency multiplication. It reduces the proportion of the jitter to the signal period and – as a result – increases the RMS voltage at the phase detector output.

The frequency multiplication is performed using the PLL circuits with the loop bandwidth judiciously chosen to the application. The bandwidth of jitter cleaner needs to be narrow to filter out the jitter, while that of jitter tracker should cover a wide jitter spectrum. As widely available PLL circuits (e.g. Texas Instruments LMK03033C used in the work) may have the bandwidth insufficient for the jitter-tracker application (because of hardware limitations), the frequency of the supplied signal is divided. As a result, the tracker discards some jitter-corrupted edges. It can be interpreted as sampling of the jitter and thus its spectrum (and also the required tracker bandwidth) may be estimated based on the frequency of the divided signal. Because of the aliasing effect, the high frequency components are shifted down to the tracker bandwidth.

The evaluation of the developed measurement device proved correctness of the theoretical assumptions. The RMS voltage from the phase comparator is linearly proportional to the jitter occurring in the signal supplied to the JMU. The obtained sensitivity and the measurement range from 5 ps up to 50 ps are satisfactory for optimizing the T&F fibre optic link performance.

Acknowledgments

This work was supported by Polish National Science Center under the decision DEC-2014/15/B/ST7/00471.

References

- [1] Riehle, F. (2017). Optical clock networks. *Nature Photonics*, 11(1), 25–31.
- [2] Kodet, J., Pánek, P., Procházka, I. (2016). Two-way time transfer via optical fiber providing subpicosecond precision and high temperature stability. *Metrologia*, 53(1), 18–26.
- [3] Predehl, K., Grosche, G., Raupach, S.M.F., Droste, S., Terra, O., Alnis, J., Legero, T., Hänsch, T.W., Udem, T., Holzwarth, R., Schnatz, H. (2012). A 920-Kilometer Optical Fiber Link for Frequency Metrology at the 19th Decimal Place. *Science*, 336(6080), 441–444.
- [4] Piester, D., Schnatz, H. (2009). Novel Techniques for Remote Time and Frequency Comparisons. *PTB-Mittellungen/Spec. Issue*, 119(2), 33–44.
- [5] Śliwczyński, Ł., Krehlik, P., Buczek, Ł., Lipiński, M. (2012). Frequency Transfer in Electronically Stabilized Fiber Optic Link Exploiting Bidirectional Optical Amplifiers. *IEEE Trans. Instrum. Meas.*, 61(9), 2573–2580.
- [6] Lipiński, M., Krehlik, P., Śliwczyński, Ł., Buczek, Ł. (2016). Testing Time and Frequency Fiber-Optic Link Transfer by Hardware Emulation of Acoustic-Band Optical Noise. *Metrol. Meas. Syst.*, 23(2), 309–316.
- [7] Śliwczyński, Ł., Krehlik, P., Kołodziej, J., Imlau, H., Ender, H., Schnatz, H., Piester, D., Bauch, A. (2017). Fiber-Optic Time Transfer for UTC-Traceable Synchronization for Telecom Networks. *IEEE Commun. Stand. Mag.*, 1(1), 66–73.
- [8] Okamoto, T., Ito, F. (2014). Laser Phase Noise Characterization Using Parallel Linear Optical Sampling. *J. Lightw. Technol.*, 32(18), 3119–3125.
- [9] Marshall, W.K., Crosignani, B., Yariv, A. (2000). Laser phase noise to intensity noise conversion by lowest-order group-velocity dispersion in optical fiber: exact theory. *Optics Letters*, 25(3), 165–167.
- [10] Cartaxo, A.V.T., Wedding, B., Idler, W. (1998). Influence of Fiber Nonlinearity on the Phase Noise to Intensity Noise Conversion in Fiber transmission: Theoretical and Experimental Analysis. *J. Lightw. Technol.*, 16(7), 1187–1194.

- [11] Śliwczyński, Ł., Krehlik, P., Salwik, K. (2016). Real-time performance monitoring of fiber optic long-distance time and RF frequency transfer link. *2016 European Frequency and Time Forum (EFTF 2016)*, 4–5.
- [12] Śliwczyński, Ł., Kołodziej, J. (2013). Bidirectional Optical Amplification in Long-Distance Two-Way Fiber-Optic Time and Frequency Transfer Systems. *IEEE Trans. Instrum. Meas.*, 62(1), 253–262.
- [13] Krehlik, P., Śliwczyński, Ł., Buczek, Ł., Kołodziej, J., Lipiński, M. (2016). ELSTAB – Fiber-Optic Time and Frequency Distribution Technology: A General Characterization and Fundamental Limits. *IEEE Trans. Ultrason., Ferroelectr., Freq. Control*, 63(7), 993–1004.
- [14] Lance, A.L., Seal, W.D., Labaar, F. (1984). Phase Noise and AM Noise Measurements in the Frequency Domain. *Infrared and Millimeter Waves.*, 11, 239–289.
- [15] Rubiola, E. (2009). *Phase Noise and Frequency Stability in Oscillators*. Cambridge University Press.
- [16] Bregni, S. (2002). *Synchronization of Digital Telecommunications Networks*. Chapter 7. John Wiley & Sons, Ltd.
- [17] Razavi, B. (2003). *Design of Integrated Circuits for Optical Communications*. Chapters 2 and 6. McGraw-Hill.
- [18] Stein, S.R. (1985). Frequency and Time – Their Measurement and Characterization. *Precision Frequency Control*, 2, 191–416.
- [19] Calosso, C.E., Rubiola, E. (2013). The Sampling Theorem in Pi and Lambda Digital Frequency Dividers. *EFTF/IFC, 2013 Joint*, 960–962.
- [20] Banerjee, D. (2006). *PLL Performance, Simulation and Design*, 4th edition. <http://www.ti.com>.
- [21] Davenport, Jr., W. B., Root, W.L. (1987). *An Introduction to the Theory of Random Signals and Noise*. IEEE Press.
- [22] Razavi, B. (1996). *Monolithic Phase-Locked Loops and Clock Recovery Circuits. Theory and Design*. A Tutorial. John Wiley & Sons, Ltd..